

Centennial changes in solar activity and the response of galactic cosmic rays

A.P. Rouillard^{*}, M. Lockwood

Space Science and Technology Department, Rutherford Appleton Laboratory, Chilton, Didcot, OX11 0QX United Kingdom

Received 30 October 2006; received in revised form 9 February 2007; accepted 11 February 2007

Abstract

There is a growing consensus that the eleven year-modulation of galactic cosmic rays (GCRs) resulting from solar activity is related to interplanetary propagating diffusive barriers (PDBs). The source of these PDBs is not well understood and numerical models describing GCR modulation simulate their effect by scaling the diffusion tensor to the interplanetary magnetic field strength (IMF). The implications of a century-scale change in solar wind speed and open solar flux, for numerical modelling of GCR modulation and the reconstruction of GCR variations over the last hundred years are discussed. The dominant role of the solar non-axisymmetric magnetic field in both forcing longitudinal solar wind speed fluctuations at solar maximum and in increasing the IMF is discussed in the context of a long-term rise in the open solar magnetic flux.

© 2007 COSPAR. Published by Elsevier Ltd. All rights reserved.

Keywords: Galactic cosmic ray modulation; Solar activity; Centennial changes

1. Introduction

The first unambiguous detection of the out-flowing solar plasma was made in 1961 by Explorer 10. Continuous recording of the near-Earth solar wind speed (V_{sw}) and its embedded magnetic field (\mathbf{B}) only started in 1963, therefore, any continuous estimates of V_{sw} or \mathbf{B} before 1963 are necessarily indirect (Lockwood et al., 1999). Svalgaard and Cliver (submitted for publication) and Rouillard et al. (2007) have shown, using geomagnetic indices, that the eleven-year running means of yearly solar wind speed values have changed by as much as $14.4 \pm 0.7\%$ between 1900 and 1950. Rouillard et al. (2007) show that the eleven-year running means of yearly averages of the total open solar magnetic flux have also changed in the same period by $73 \pm 5\%$ leading to a $45.1 \pm 4.5\%$ change in the strength of the interplanetary magnetic field at Earth. Similar estimated changes in \mathbf{B} and V_{sw} are obtained using three differ-

ent combinations of geomagnetic indices [For details of the method, the reader is referred to Rouillard et al. (2007).].

Further evidence for secular change in the heliosphere comes from direct measurements of Galactic Cosmic Ray (GCR) fluxes and the abundances of cosmogenic isotopes produced by GCR bombardment and stored in terrestrial reservoirs, such as ice sheets, tree trunks and ocean sediments. The Dye-3 ice core from Greenland shows century-scale drift in the ^{10}Be cosmogenic isotope, whereas much smaller changes are seen in an Antarctic core. In general, the Dye-3 data are the more reliable because local precipitation rates are much greater. In addition, Dye-3 agrees more closely with ^{14}C found in tree trunks all over the world up until about 1940, after which increased release of carbon from fossil fuel burning and nuclear bomb explosions render the ^{14}C record unusable. Lockwood (2001, 2003) investigated the relationship between GCR changes and the secular change in the open solar flux using regression and response function analysis. In the present paper, we investigate this relationship quantitatively considering the physical mechanisms that may be active.

^{*} Corresponding author.

E-mail address: alexisrouillard@yahoo.co.uk (A.P. Rouillard).

In the second section of this paper, we describe the secular magnetohydrodynamic changes of the solar wind inferred by geomagnetic activity in the last hundred years. The changes discussed are the in-ecliptic V_{sw} and \mathbf{B} changes and an attempt is made to derive solar wind changes valid for the entire heliosphere in the third section. Secular changes in the population of transients such as coronal mass ejections and interaction regions are also discussed in light of recent papers. In the fourth section of this paper, we will investigate the implications of the MHD changes discussed above on the propagation of galactic cosmic rays (GCRs) using a 1-D GCR modulation model and will show the inadequacy of a 1-D model to derive secular changes in GCRs. Finally we propose additional modulation mechanisms which should be accounted for in deriving GCR intensities back in time in Section 5.

2. Secular near-Earth solar wind changes

Fig. 1 shows the secular changes in the interplanetary magnetic field (IMF) strength (panel a) and the solar wind speed (panel b), both derived using the combination of two different geomagnetic indices (Rouillard et al., 2007), a method first proposed by Svalgaard and Cliver (submitted for publication). The eleven-year running means of the IMF strength and solar wind speed are also plotted on top of the annual values. The inverted eleven-year running means of cosmic ray counts measured by the Climax neu-

tron monitor are fitted to the interplanetary magnetic field \mathbf{B} in panel (a) using black dots and show a clear anti-correlation with the eleven-year running mean of the IMF strength.

The average solar wind speed increase seen in panel b of Fig. 1 is to be expected, given the rise in open solar flux. This is because the increasing quantity of open field lines threading the source surface (taken to be a sphere centered at the Sun's center with radius 2.5 solar radii) will decrease the average expansion rate of flux tubes between the photosphere and the source surface. According to the Wang/Sheeley empirical law (Wang and Sheeley, 1990), this will increase the average wind speed. This is a global change in wind speed (Effect 1).

An alternative interpretation is that the increase in average wind speed at Earth is related to a more frequent occurrence of polar coronal hole extensions and, at solar maximum, isolated coronal holes in the ecliptic regions. These increases are due, respectively, to larger polar coronal holes at solar minimum and more open field line footprints spread over the entire surface at solar maximum. These more prominent coronal holes increase the probability that the Earth intersects fast flow streams (Effect 2).

We have information about Effect 2 at all solar latitudes in the modern era from potential field source surface (PFSS) extrapolations of Carrington maps of the corona derived from photospheric magnetograms (see discussion in Section 2). However, we have no ready source of

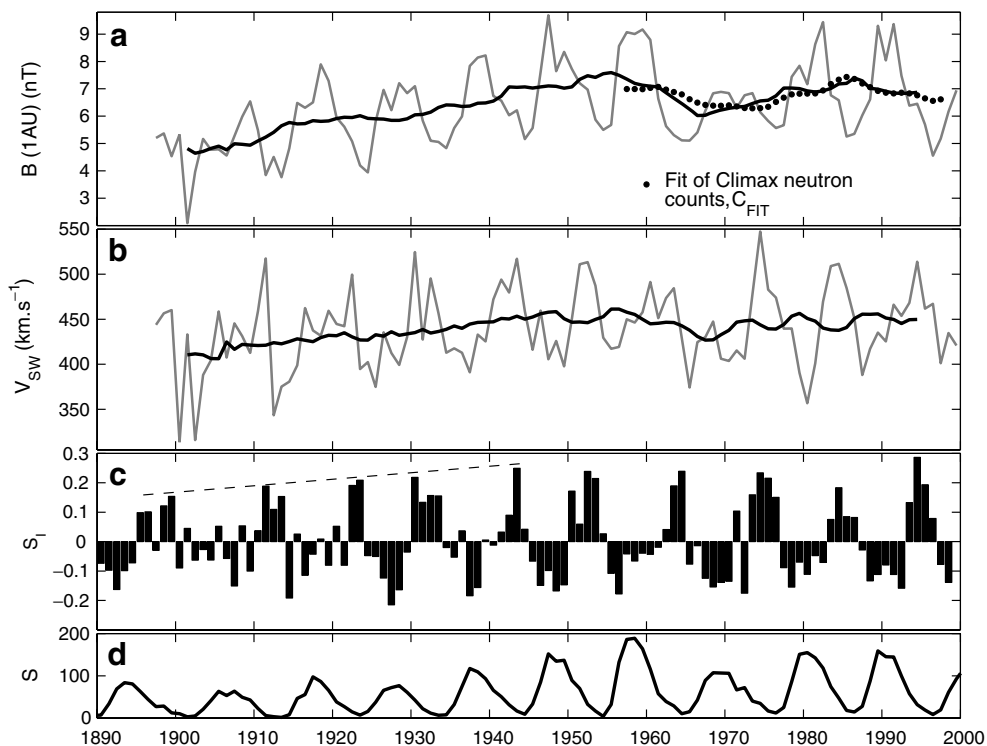


Fig. 1. Panel a: the variation of the IMF strength, B , at Earth inferred from the median and corrected aa_c geomagnetic indices, panel b: the variation of the solar wind speed V_{sw} derived the same way, panel c: the detrended Sargent recurrence index (S_i) derived from aa_c . panel d: the variation of the international sunspot number (S). The dotted line in panel a gives the eleven-year running means of C_{fit} , the best linear fit of the Climax neutron monitor counts C , to B .

information on this before 1966 and the most reliable solar magnetograms are only available after 1976.

Also shown is the Sargent Recurrence Index (SRI, labelled S_1) (panel c) and the international sunspot number (S) (panel d). SRI is calculated from the wind speed-dependent aa_c , geomagnetic index; this is the aa index which has been corrected for magnetometer calibration errors by Lockwood et al. (in press). SRI is a running mean of the autocorrelation of aa_c lagged by 27.27 days (the solar rotation rate as seen from Earth) and indicates the occurrence of recurring fast streams in the ecliptic plane. We here correct for periods of low activity (which tend to autocorrelate) by detrending the data with an eleven-year running mean.

The large peaks in SRI correspond to high-speed wind, emitted by polar coronal hole extensions in the declining phases of the solar activity cycle and sporadic short-lived isolated coronal holes at low latitudes during solar maximum. The alignment of fast wind after slow wind due to solar rotation leads to the formation of so-called Co-rotating Interaction Regions (CIRs) which trigger geomagnetic activity. Cliver et al. (1996) have shown that the peaks on the declining phases of solar activity are visible in geomagnetic activity with a 22-year cycle in magnitude and duration, a feature associated with polar coronal hole formation and the increased occurrence of equatorial CIRs (Cliver et al., 1996). There is also a pronounced odd–even (Hale) cycle effect in both the IMF strength and the occurrence of active longitudes relative to the more regular sunspot cycle (not shown here) which affect the duration of solar activity minima with ‘shorter solar minima’ after odd cycles (Wang et al., 2006; Rouillard and Lockwood, in press).

As seen in Fig. 1, the $45.1 \pm 4.5\%$ increase in the IMF strength and the $14.4 \pm 0.7\%$ increase in solar wind speed deduced from ground-based magnetometers between 1903 and 1956 are accompanied by an increase in the recurrence peaks in SRI during successive declining phases. These peaks being associated with recurring wind streams, we can infer an increase in the occurrence of CIRs from one solar minimum to the next during this interval. The increase in the yearly averages of solar wind speed (panel b) are therefore partly related to more frequent interactions of the magnetosphere with CIRs (Effect 2). S_1 characterises only the changes in recurrence in the ecliptic plane. Rouillard and Lockwood (in press) demonstrated how, while CIRs are limited to a range of latitudes $[-30^\circ:30^\circ]$ at sunspot minimum, they occur over a much greater range of latitudes during solar maximum years when the Heliospheric Current Sheet (HCS) displays large latitudinal excursions. Hence many solar maximum CIRs are not recorded by S_1 . Moreover, the large photospheric activity during solar maximum forces isolated coronal holes to change location and morphology in the space of one rotation, therefore making a clear 27-day recurrent pattern difficult to detect.

Finally, it should be noted that Cliver and Ling (2002a) and Wang et al. (2006) find a high correlation between the

number of CMEs, sunspot number variations and an anti-correlation with GCRs. In particular, the subset of fastest CMEs measured is highly anti-correlated with the variation of GCRs (Wang et al., 2006). This subset of fast CMEs is more likely to coalesce with CIRs and form the globally merged structures studied by Burlaga and Ness (1994). A steady increase in sunspot number during the last hundred years has very probably led to larger cycles of CME occurrence. Thus the inferred fall in GCR fluxes between 1903 and 1956 (see the next sections) probably occurred while there was an increase in the number of CMEs at successive solar maxima in conjunction with an increase in the number of CIRs at solar minima (as inferred from S_1). We here classify CMEs, CIRs, or any other barriers capable of depleting the heliosphere from GCRs by compressing magnetic field, as propagating diffusive barriers (PDBs).

3. MHD secular changes in the heliosphere

3.1. The magnetic field

The increase in IMF strength and solar wind speed inferred by geomagnetic indices reflects changes of the in-ecliptic solar wind. To extract changes occurring in the global heliosphere for our discussion of GCR modulation, we use the method of Lockwood et al. (1999) subsequently refined by Rouillard et al. (2007). The latitudinal isotropy of the average radial IMF component ($B_r|_{T=1 \text{ day}}$), as measured by Ulysses (Balogh et al., 1995) means that the total open solar magnetic flux $F_s|_T(t) = (4\pi B_r|_T(t) R_{1 \text{ AU}}^2)/2$ is for a particular time t a heliospheric invariant. Lockwood et al. (2004) show that this equation is valid to a few percent for averages over 27 days or longer. To obtain the best match to PFSS data, the absolute value of B_r should be taken over a timescale $T = 1$ day (Lockwood et al., 2006). The validity of Parker spiral theory over yearly averages (Forsyth et al., 1996) allows us to combine the average IMF strength $B(t)$ and the solar wind speed $V_{sw}(t)$ shown in Fig. 1 to obtain the variation of average $B(r)|_{T=1 \text{ hour}}$ and hence the total flux $F_s(t)|_{T=1 \text{ hour}}$ at 1 AU:

$$F_s|_{T=1 \text{ hour}}(t) = 2\pi R_{1 \text{ AU}}^2 B(t) \cos[\arctan(R_{1 \text{ AU}}\omega/V_{sw}(t))], \quad (1)$$

where ω is the angular rotation rate of the Sun. Rouillard et al. (2007) find a strong linear relation between averages of F_s for $T = 1$ day and 1 hour. The regression fit can be used to correct for the continuously removed open flux as well as the newly-opened field lines and short-lived distortions from Parker spiral field orientation which are recorded in hourly averages but cancelled in the signed daily averages of B_r , $|B_r|_{T=1 \text{ day}}$ (see Rouillard et al. (2007) for details of the procedure). The Archimedean field at all latitudes in the heliosphere can then be obtained by applying Parker spiral theory in 2D: $B(r, \lambda, t) = F_s|_{T=1 \text{ day}}(r/2\pi)^{1/2} [1 + (r\omega \cos(\lambda)/V_{sw}(t))^2]^{1/2}$. The derived total open flux is

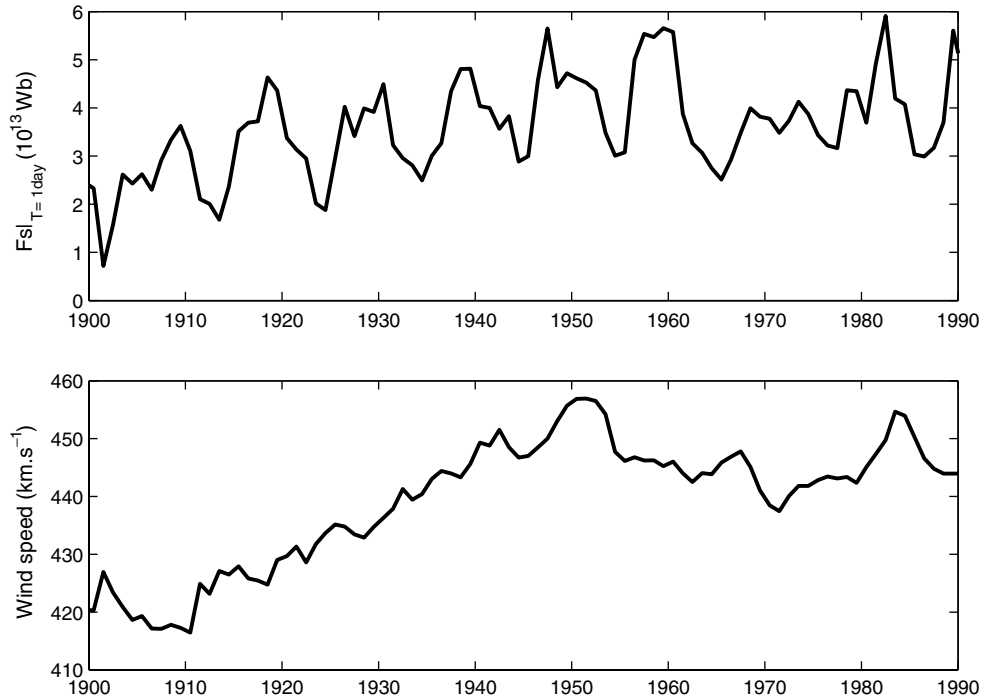


Fig. 2. Top panel: the variation of the total open flux derived from Eq. (1). Bottom panel: the variation of the 22-year running means of the solar wind speed in the ecliptic.

plotted in the top panel of Fig. 2 and will be used to discuss GCR modulation.

3.2. The solar wind plasma speed

The Ulysses mission has revealed that the highly fluctuating solar wind speed which we experience in the ecliptic is very different to the more persistent fast streams at high latitudes, in particular during sunspot minimum. PFSS predictions of solar wind speed show that the flux tubes of polar coronal holes are the source of high speed streams in the very high latitudes and the source of slower wind when expanding super-radially above the streamer belt. The emergence of sunspots in the streamer belt region forces longitudinal fluctuations of the solar wind speed which allow fast and slow flow in the ecliptic. The highly regular field line topology of solar minimum is lost at sunspot maximum so that no topology could be inferred from in-ecliptic wind speed estimates before the continuous recording of solar magnetograms (1966). In other words, we do not have an equivalent of the solar radial magnetic field isotropy for the solar wind speed. We here look at the implications of the Effect 1 (discussed in Section 2) acting in isolation (i.e. a mean unstructured rise in solar wind speed). The solar cycle variation of the solar wind speed derived using geomagnetic activity is specific to the Earth's latitude. To simulate an unstructured average change in solar wind speed for the entire heliosphere, we remove this solar cycle variation by taking a 22-year running mean shown in the bottom panel of Fig. 2 which in the next section we assume to apply to the whole heliosphere. Ideally, one would estimate the evolution of the solar wind at all

latitudes for the 10 cycles between 1900 and 2000, a task that is beyond the scope of this paper.

Whang et al. (2003) have shown that the location of the termination shock responds to changes in solar wind properties at 1 AU (such as the solar wind speed). Solar cycle variations of the termination shock location are predicted of amplitude 20–30% in the ecliptic and 66% in the high latitude regions. They argue that the solar wind speed V_{sw} and temperature T beyond 60 AU can be approximately related to the solar wind speed at 1 AU at the same heliographic latitude. Hence changes of 14% between 1903 and 1956 in wind speed (which represents half a typical solar cycle variation in the modern era) will have profound effects on the temperature and speed of the solar wind in the inner and outer heliosphere as well as on the location of the termination shock.

4. Cosmic ray modulation

4.1. Cosmic ray transport model

In terms of GCR modulation there are two major consequences of the phenomenological changes: a decrease in the size of the modulation region and the degree to which GCRs are advected during their transport to the Earth. This is readily seen in the modulation approximation made by Parker (1965) using a Fokker–Planck equation:

$$\frac{\partial f}{\partial t} = \frac{\partial}{\partial x_i} \left[\kappa_{ij}^S \frac{\partial f}{\partial x_j} \right] - \mathbf{V}_{sw} \cdot \nabla f + \frac{1}{3} \nabla \cdot \mathbf{V}_{sw} \left[\frac{\partial f}{\partial \ln p} \right] + Q, \quad (2)$$

where the terms in the right hand side correspond to diffusion, advection, adiabatic cooling or heating and any local

source Q . κ_{ij}^S is the symmetric part of the diffusion tensor and V_{sw} is the solar wind velocity. The adiabatic cooling term is expressed in terms of the rate of change of the omni-directional distribution function with respect to the logarithm of the momentum p of the particle. We note that there is also an anti-symmetric part in the diffusion tensor usually associated with gradient and curvature drifts in the large-scale dipolar heliosphere which have a large effect when solar activity diminishes.

The centennial decrease in the production of ^{10}Be trapped in ice-cores (McCracken et al., 2004a) related to decreasing levels of cosmic ray flux at Earth is usually associated with the increase in open solar magnetic flux shown in Fig. 2 (Lockwood et al., 1999), or the IMF strength (Caballero-Lopez et al., 2004) affecting the diffusion tensor.

Part of the decrease could also be related to an increasing region of modulation but the short lags between GeV proton fluxes and IMF parameters at Earth show a large part of the shielding takes place in the inner-heliosphere close to the Earth (Cane et al., 1999; Rouillard and Lockwood, 2004). Hence we here neglect this effect.

In terms of cosmic ray modulation, the change in the number of CIRs and CMEs from one cycle to the next will lead to changes in the scattering level in successive solar minima/maxima preventing cosmic rays from recovering. Application of quasi-linear theory to the scattering of galactic charged particles on random background of magneto-static fluctuations relates the diffusion tensor to some power of the fluctuating magnetic field correlation length (l_c), the square of the strength of the local field (B^2) and the inverse square of the field variance (σ^{-2}). As noted by Caballero-Lopez et al. (2004) and Burlaga and Ness (1994) find that the measured magnetic field variance both in the in-ecliptic and in the outer heliosphere is proportional to the strength of the IMF at 1 AU so that the strongest dependence of the diffusion coefficients is to the correlation length which could have a B^{-n} dependence with $n \in [1:3]$. The range of the exponent arises from the effect associated with PDBs (CMEs, CIRs) in the heliosphere. It is clear that the variation of the number of these transients during the solar cycle will lead to solar cycle variations in the dependence of the correlation length on B , (i.e. changes in n). We assume in this model that n remained unchanged over the last hundred years: in other words, a secular change in the occurrence of interaction regions occurred together with any related change such that the correlation length dependence on B was unchanged. We do not know how PDBs have evolved between 1903 and 1956 so we assume that both have evolved in the same proportion. In this way, we allow for Effect 2 discussed in Section 2, through the occurrence of PDBs.

The effect of the secular changes shown in Fig. 2 in solar activity on GCRs is now investigated by solving Eq. (2) numerically with various degrees of approximation. Our ignorance of the exact evolution of coronal holes and the HCS tilt during the period of interest (1903–1956) means that we here solve for a spherically symmetric heliosphere

to avoid false assumptions. This simplistic model is used to investigate whether the increase in open flux can explain the long-term change in GCRs. Discrepancies between predictions and observations are discussed in the last part of this paper.

A spherically symmetric heliosphere means that the anti-symmetric and symmetric parts of the diffusion tensor are integrated in a single 'effective diffusion coefficient' calibrated against modern data by solving the full time-dependent transport equation. The interstellar spectrum is taken from Webber and Lockwood (2001) as $f_{LIS} = 21.1T^{-2.8}/(1 + 5.85T^{-1.22} + 1.18T^{-2.54})$, where T is the kinetic energy in GeV and fixed at 100 AU. The solar wind speed is assumed to be given by panel b of Fig. 2. Ideally, a 2-D or 3-D model would evaluate \mathbf{B} at all points on the grid obtained by using Eq. (1) but this requires knowledge of the full 3-D evolution of the solar wind speed. Here, we consider the open flux variation which is assumed to be a reliable quantification of the level of turbulence and the number of scattering centers in the entire heliosphere. Hence the variation of the number of CMEs and CIRs leading to global merged interaction regions is assumed to be a function of the open flux. The diffusion coefficient κ is hence taken simply as $\kappa = \alpha(\gamma/F_s)^n$ where F_s is in 10^{14} Wb, $\alpha = 4 \times 10^{22} \beta P$ where P is the rigidity of the particle considered with β the speed of the particle in terms of the speed of light and the value of $\alpha = 4 \times 10^{22} \text{ cm}^2 \cdot \text{s}^{-1}$ and $\gamma = 2.67$ are obtained by comparing the solar minimum GCR spectrum of 1997 obtained by IMP8 and the spectrum obtained by the present numerical solution. The counting rate for Mount Washington neutron monitor is obtained by integrating the product of the neutron (production rate) response function times the intensity prediction at 1 AU for all the rigidities above the lower low-rigidity cut-off of 1.02 GV.

4.2. GCR observations and 1-D model predictions

Fig. 3 compares the predicted count-rates to the measured rates at Mount Washington (1953–1992) and Climax (1992–2001). We find a best fit of the predicted variation to the measured neutron monitor data for $n = 1.8$.

The centennial change in GCR predicted by this scaling of the diffusion coefficient and the variation in solar wind speed is compared to the Neher (crosses) and Forbush data (histogram before 1965) gathered and intercalibrated by McCracken and Heikkila (2003) for the years preceding 1963. The Neher ionisation data has been accurately calibrated to within a few percent (McCracken and Heikkila, 2003). The ionisation dataset is however unique and cannot be given the level of accuracy of the world-wide network of modern neutron monitors which can be cross-checked. It is clear that, while the neutron monitor data is approximately simulated (1963–2000), the data for (1933–1953) cannot be explained by the change in open flux and solar wind speed in isolation. There is a systematic offset between the prediction and the Neher dataset for 1933–1963. The difference

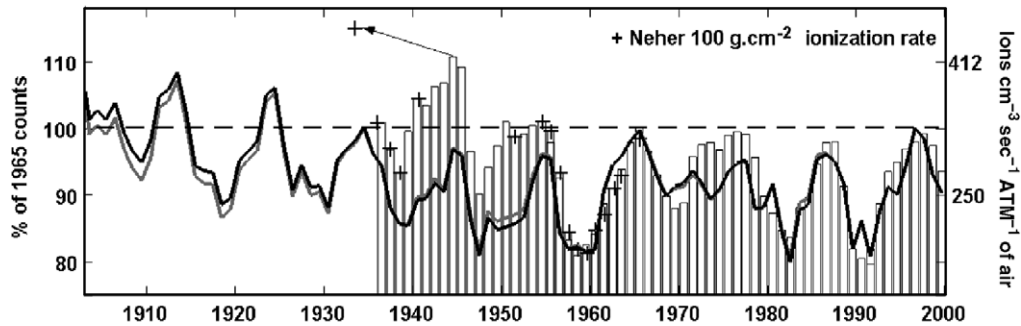


Fig. 3. The histograms show the GCR flux variation recorded by the Mount Washington neutron monitor (1965–1991) and the Climax neutron monitor (1991–2000). The histogram before 1965 shows the Forbush data calibrated onto the Neher data shown as crosses by McCracken and Heikkila (2003). The results of the spherically symmetric GCR modulation model are shown for the inferred change in wind speed (black curve) and no change in wind speed (grey curve).

between the 1933 and 1948 peaks (solar minima) is the same (black vector) as the predicted change but the absolute levels are different. As noted by McCracken et al. (2004b), a large change in the influence of gradient and curvature drifts could have affected the link between absolute open flux values and GCR in 1954 relative to 1963. For instance, there is a growing consensus that cycle 20 (1968–1973) cannot be modelled without including the effect of gradient and curvature drifts (Rouillard and Lockwood, 2004) and cycle 20 is badly modelled in this spherically symmetric model. For comparison, we also plot in Fig. 3 the change in GCR fluxes over the last hundred years if the solar wind speed had not changed (grey curve) and had the present value at all times. For this low rigidity cut-off the change in wind speed has an effect by both affecting the level of advection and adiabatic cooling but this effect is small compared to that needed to explain the drift in the early ionisation chamber data of Forbush and Neher.

Hence, the 1-D spherically symmetric model cannot explain the long-term drift in the early cosmic ray data, nor in cosmogenic isotope abundances such as ^{10}Be which show drifts consistent with the Neher data (McCracken et al., 2004a).

5. Possible causes of the 1944–1954 decrease in GCRs

Fig. 3 shows that the variation in the open flux and solar wind speed, as inferred and used in this paper, cannot explain the change in intensity of GCRs before 1960. We note that it is a lack of a similarly rapid change in F_S between 1944 and 1954 which causes the discrepancy. This pronounced change in GCR intensity is also seen in ^{10}Be (see paper by McCracken (2007)). There is a large change in the dependence of the diffusion tensor to the open flux during this period which could be due to latitudinal effects. The necessity to include the latitudinal dimension in GCR modulation results from the latitudinal distribution of solar wind speed throughout the solar cycle and the organised distribution of the heliospheric field, in particular at solar minimum. A question related to the GCR intensity change between the 1944 and

1954 minima is the ability of the heliosphere to keep the level of GCRs lower in the last four minima.

Inspection of Fig. 3 in the paper by Foster and Lockwood (2001) shows that since 1954 by the standard deviations of sunspot group latitudes has been roughly the same during the last four minima (1964, 1975, 1986, 1996) and higher than the solar minima preceding 1964. Their data is plotted in panel c of Fig. 4 as percentage values of the 1965 value. Also plotted, in panels a and b, respectively, are the cosmic ray variations (as shown in Fig. 3) and the open flux derived from geomagnetic activity (as shown in Fig. 2). The black vectors show the difference between the changes of the three parameters in the course of these three minima 1933, 1944 and 1954. We see that the open flux has not changed between 1944 and 1954 whereas the spread in sunspot latitude has increased. Hence the latitudinal extent of the streamer belt during the 1954 minimum, which is dictated by sunspot and coronal field emergence, might have not been able to reach the 1944 minimum extent. The HCS tilt angle is fitted onto the standard deviation of sunspot latitudes for comparison. It is not intended to establish a linear link in doing so, but rather to show that both parameters have evolved together in the recent decades. The minimum extent of the HCS tilt has been 10° since 1978 and the latitudinal extent of the surrounding slow flow extended to $\pm 25\text{--}30^\circ$ during these periods. Very flat current sheets can be seen in eclipse images of 1954 for instance (Cliver et al., 2002b). There are two implications of the possible evolution of the width of the streamer belt inferred by the sunspot spread.

Firstly, the importance of gradient and curvature drifts is usually scaled to the width of the streamer belt. The large implied decrease between 1944 and 1954 and the low level of GCRs since the 1954 minimum could be related to a sudden change in the importance of gradient/curvature drifts during recent minima. Gradient and curvature drifts set the flow pattern of GCRs in the heliosphere, the pattern being reversed every eleven years when the dipole field reverses. GCRs are either forced to propagate along a turbulent current sheet or along a turbulent polar field during successive solar cycles.

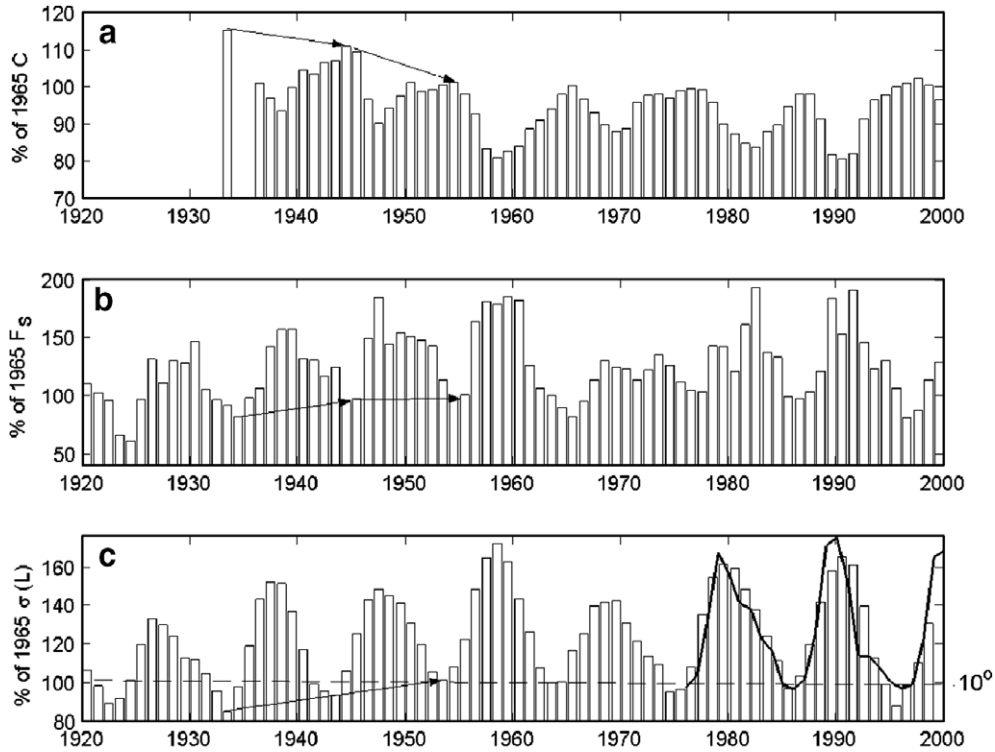


Fig. 4. Panel a: the variation of GCR counts (C) assembled as in panel a of Fig. 3. Panel b: open flux (F_s) derived from geomagnetic activity expressed as a percentage of the value in 1965. Panel c: the standard deviation of sunspot latitudes ($\sigma(L)$) expressed as percentage values of 1965. Black vectors mark the changes in the three parameters between the solar minima of 1933, 1944 and 1954. The latitudinal excursions of the HCS tilt (solid black line) are fitted onto the standard deviations of sunspot latitudes histograms. The minimum latitudinal extent of the HCS between 1978 and 1999 is shown by a dotted line and is 10° .

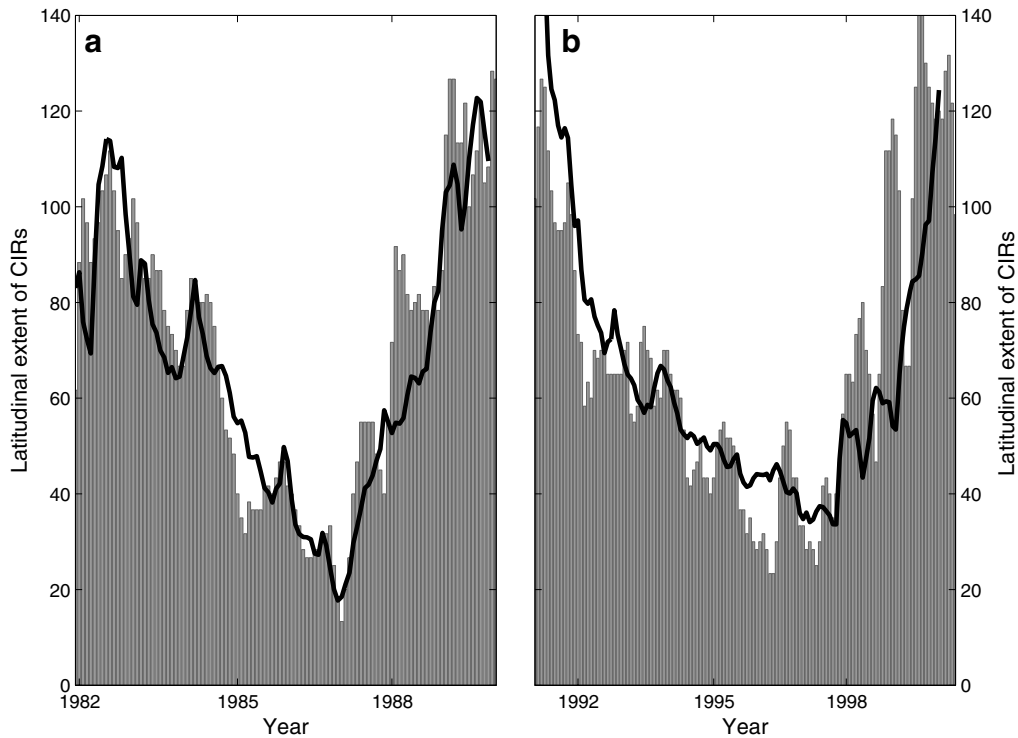


Fig. 5. The variation of the latitudinal excursions of interaction regions (grey histograms) predicted from potential field source surface extrapolation (Rouillard and Lockwood, in press) for the 1987 (panel a) and 1997 (panel b) solar minima. The inverted fitted GCRs counts from the Climax neutron monitor are also shown in black for comparison.

Secondly, Rouillard and Lockwood (in press) have recently argued that the heliosphere never rests in the recent solar minima because of the continuous formation of CIRs. They show how the level of open flux rooted in the low latitude regions of the photosphere, together with the latitudinal excursion of the HCS, dictates the formation of CIRs in the heliosphere and hence the degree to which interplanetary magnetic field lines are compressed and dragged out. Fig. 5 shows the variation of the added unsigned north and south latitudinal excursions of IRs which have a ratio of 1.7 between fast and slow flow (large compression of \mathbf{B} field). This estimation of the latitudinal variation of CIRs was obtained using potential field source surface model (Rouillard and Lockwood, in press). The analysis is made by propagating the wind speed predicted by the Wang/Sheeley empirical law and is confirmed by complete MHD models of the corona for overlapping intervals of time. The variation of these PDBs gives the highest correlation with GCR variations (Rouillard and Lockwood, in press) during recent minima of opposite solar polarity. We expect a drift-induced propagation of GCRs protons along the HCS in panel a of Fig. 5 hence the anti-correlation with GCRs is higher ($cc = -0.86$) than for panel b ($cc = -0.76$).

The changes in the importance of drifts and in the latitudinal extent of solar minima CIRs from pre-1954 solar minima conditions to modern solar minima could have induced the large change in the relation between the diffusion tensor and the open flux.

Concerning solar maxima, the large change between 1948 and 1957 in GCR fluxes was occurring during a large change in sunspot number (but without a correspondingly large change in open flux) which reached a peak in 1954, hence, if the correlation between CMEs and sunspots seen in the last cycles pertained during the first half of the 20th century, CME numbers should have increased dramatically between solar maxima in 1948 and 1958 (unlike the open flux). We stress, however, that the relative roles of CMEs and CIRs in cosmic ray modulation is still a matter of debate.

6. Conclusion

We have discussed the rise in the open flux and the solar wind speed between 1903 and 1956. The recurrence index, S_1 , derived from geomagnetic data shows us that the solar wind speed change has been accompanied by a rise in the number of CIRs in the ecliptic plane. These changes mean that the heliosphere was very different at the beginning of the 20th century. In particular, the level of scattering in the recent solar minima due to CIRs never goes to zero. Application of a spherically symmetric heliosphere in the study of long-term changes in GCR intensity at 1 GV by solving the Parker transport equation has been proven inadequate. In particular, the change in GCR intensity between 1944 and 1954 cannot be explained by simply scaling the diffusion coefficient to the open flux. A 3-D model is

therefore necessary with the correct integration of the latitudinal extent of the HCS which dictates particle drifts in the heliosphere as well as the latitudinal extent reached by interaction regions throughout the solar cycle. The difference of CMEs rate evolution and open flux could also lead to a change in the relation between open flux and the diffusion tensor.

Acknowledgements

We thank Yi-Ming Wang of the Naval Research Laboratory for providing the PFSS data. This work was funded by the National Environment Research Council (NERC, UK) and the Science and Technology Facilities Council (STFC, UK). The OMNI-2 interplanetary magnetic field and solar wind flow data was compiled by the NASA/Goddard Space Flight Center, Space Physics data facility and distributed by the World Data Center, STFC, Chilton, UK.

References

- Balogh, A., Smith, E.J., Tsurutani, B.T., Southwood, D.J., Forsyth, R.J., Horbury, T.S. The heliospheric magnetic field over the south polar region of the Sun. *Science* 268 (5213), 1007–1010, 1995.
- Burlaga, L.F., Ness, N.F. Merged interaction regions and large-scale magnetic field fluctuations during 1991: Voyager 2 observations. *Journal of Geophysical Research* 99, 19341–19350, 1994.
- Caballero-Lopez, R.A., Moraal, H., McCracken, K.G., McDonald, F.B. The heliospheric magnetic field from 850 to 2000 AD inferred from ^{10}Be records. *Journal of Geophysical Research* 109, A12, 2004.
- Cane, H.V., Wibberenz, G., Richardson, I.G., von Roseninge, T.T. Cosmic ray modulation and the solar magnetic field. *Geophysical Research Letters* 26 (5), 565–568, 1999.
- Cliver, E.W., Boriakoff, V., Bounar, K.H. The 22-year cycle of geomagnetic and slow wind activity. *Journal of Geophysical Research* 101 (A12), 27091–27109, 1996.
- Cliver, E., Ling, A. Coronal mass ejections, open magnetic flux, and cosmic ray modulation. *Astrophysical Journal* 556, 432–437, 2002a.
- Cliver, E.W., Svalgaard, L., Ling, A.G. Evidence for a Dominant Russell-McPherron/Rosenberg-Coleman Origin of the Semiannual Variation of Geomagnetic Activity in 1954 and 1996, AGU, American Geophysical Union, Fall Meeting 2002, abstract SM72B-0614, 2002b.
- Forsyth, R.J., Balogh, A., Horbury, T.S., Erds, G., Smith, E.J., Burton, M.E. The heliospheric magnetic field at solar minimum: Ulysses observations from pole to pole. *Astronomy and Astrophysics* 316, 287–295, 1996.
- Foster, S., Lockwood, M. Long-term changes in the solar photosphere associated with changes in the coronal source flux. *Geophysical Research Letters* 28, 1443–1446, 2001.
- Lockwood, Stamper, M.R., Wild, M.N. A doubling of the Sun's coronal magnetic field during the last 100 years. *Nature* 399, 437–439, 1999.
- Lockwood, M. Long-term variations in the magnetic fields of the Sun and the heliosphere: their origin, effects, and implications. *Journal of Geophysical Research* 106, 16021–16038, 2001.
- Lockwood, M. Twenty-three cycles of changing open solar magnetic flux. *Journal of Geophysical Research* 108, 1128–1143, 2003.
- Lockwood, M., Forsyth, R.B., Balogh, A., McComas, D.J. Open solar flux estimates from near-Earth measurements of the interplanetary magnetic field: comparison of the first two perihelion passes of the Ulysses spacecraft. *Annales Geophysicae* 22, 1405–1935, 2004.
- Lockwood, M., Whiter, D., Hancock, B., Henwood, R., Ulich, T., Linthe, H.J., Clarke, E., Clilverd, M.A. The long-term drift in geomagnetic

- activity: calibration of the *aa* index using data from a variety of magnetometer stations, *Annales Geophysicae*, in press.
- Lockwood, M., Rouillard, A.P., Finch, I.D., Stamper, R. Comment on 'The IDV index: its derivation and use in inferring long-term variations of the interplanetary magnetic field strength' by Svalgaard and Cliver. *Journal of Geophysical Research* 111, A09109, 2006.
- McCracken, K.G., Heikkila, B., The cosmic ray intensity between 1933–1965, 28th Cosmic Ray Conference, Tsukuba, Japan, vol. 7, pp. 4117–4120, 2003.
- McCracken, K.G., McDonald, F.B., Beer, J., Raisbeck, G., Yiou, F. A phenomenological study of the long-term cosmic ray modulation 850–1958 AD. *Journal of Geophysical Research* 109, 2004a.
- McCracken, K.G., Beer, J., McDonald, F.B. Variations in the cosmic radiation, 1890–1986, and the solar and terrestrial implications. *Advances in Space Research* 24, 397–406, 2004b.
- McCracken, K.G. Changes in the cosmic ray and heliomagnetic components of space climate, 1428–2005, including the variable occurrence of solar energetic particle events, *Proc. ISSC2*, 109 (A12), Cite ID A12103, 2007.
- Parker, E.N. The passage of energetic charged particles through interplanetary space. *Planetary & Space Science*, 9–49, 1965.
- Rouillard, A.P., Lockwood, M. Oscillations in the open solar magnetic flux with period 1.68 years: imprint on galactic cosmic rays and implications for heliospheric shielding. *Annales Geophysicae* 46 (22), 4381–4395, 2004.
- Rouillard, A.P., Lockwood, M., Finch, I.V. Centennial changes in the solar wind speed and in the open solar flux. *Journal of Geophysical Research* 112 (A5), A05103, doi:10.1029/2006JA012130, 2007.
- Rouillard, A.P., Lockwood, M. Solar wind speed response to enhancements of the non-axisymmetric field: consequences for cosmic ray modulation, *Astronomy & Astrophysics*, in press.
- Svalgaard, L., Cliver, E.W. The Solar wind during Grand Minima, Long-term Changes in the Sun and their Effects in the Heliosphere and Planet Earth, Sanai, Romania, 13–16 September, 2006, *Advances in Space Research*, doi:10.1016/j.asr.2007.06.066.
- Wang, Y.M., Sheeley, N.R. Magnetic flux transport and the sunspot-cycle evolution of coronal holes and their wind streams. *Astrophysical Journal* 365, 372–386, 1990.
- Wang, Y.M., Sheeley, N.R., Rouillard, A.P. Role of the Sun's nonaxisymmetric open flux in cosmic-ray modulation. *The Astrophysical Journal* 644 (1), 638–645, 2006.
- Whang, Y.C., Burlaga, L.F., Wang, Y.M., Sheeley, N.R. Solar wind speed and temperature outside 10 AU and the termination shock. *Astrophysical Journal* 589, 635–643, 2003.
- Webber, W.R., Lockwood, J. Voyager and Pioneer spacecraft measurements of cosmic ray intensities in the outer heliosphere; toward a new paradigm for understanding the global modulation process; 1, Minimum solar modulation (1987 and 1997). *Journal of Geophysical Research* 106, 29333–29340, 2001.